




# Evaluation of exposure factors of dual-energy contrast-enhanced mammography to optimize radiation dose with improved image quality

Acta Radiologica Open  
11(8) 1–8  
© The Author(s) 2022  
Article reuse guidelines:  
[sagepub.com/journals-permissions](https://sagepub.com/journals-permissions)  
DOI: 10.1177/20584601221117251  
[journals.sagepub.com/home/arr](https://journals.sagepub.com/home/arr)  


Sachila Niroshani<sup>1,2</sup> , Tokiko Nakamura<sup>1,3</sup> , Nikaidou Michiru<sup>1</sup> and Toru Negishi<sup>1</sup>

## Abstract

**Background:** Dual-energy contrast-enhanced mammography (DECEN) is an advanced breast imaging technique of digital mammography.

**Purpose:** To assess the total radiation dose received from complete DECEN using different combinations of exposure parameters for low- and high-energy images.

**Materials and methods:** A dedicated phantom with three different concentrations of iodine inserts was used. Each iodine insert was 10 mm in diameter and concentration of 1.0 mgI/cm<sup>3</sup>, 2.0 mgI/cm<sup>3</sup>, and 4.0 mgI/cm<sup>3</sup>. The phantom was exposed at varying kVp levels. Mean glandular dose (MGD) was estimated. Contrast to noise ratio (CNR) and figure of merit (FOM) of the iodine inserts were used to assess the image quality.

**Results:** The optimum CNR of the recombined images was obtained by using 28 kVp + 49 kVp tube voltage combination for 50 mm thickness, 50% fibroglandular phantom only with a 26% dose increase compared to the highest voltages (32 kVp + 49 kVp) that can be used for low energy (LE) and high energy (HE) imaging. The CNR value was increased with increasing iodine concentration ( $R^2 > 0.99$ ).

**Conclusion:** The use of as low as possible tube voltage for the LE imaging of standard 50% fibroglandular–50% adipose, 50 mm thickness breast while using the highest tube voltage for HE imaging has reduced the MGD while keeping optimum image quality.

## Keywords

Dual-energy contrast-enhanced mammography, low energy, high energy, radiation dose

Received 3 May 2022; accepted 15 July 2022

## Introduction

The conspicuity of the lesion is reduced in dense breasts when imaged with conventional mammography.<sup>1</sup> Therefore, at the next level, mammography uses iodinated contrast media to enhance breast cancer.<sup>2</sup> The technique uses the advantage of differential attenuation at the k absorption edge of iodine (33.169 keV).<sup>3</sup> Dual-energy contrast-enhanced mammography (DECEN) is an advanced breast imaging technique of digital mammography.<sup>4,5</sup> In dual-energy technique, two images were acquired at

<sup>1</sup>Department of Radiological Sciences, Graduate School of Human Health Sciences, Tokyo Metropolitan University, Tokyo, Japan

<sup>2</sup>Department of Radiography and Radiotherapy, Faculty of Allied Health Sciences, General Sir John Kotelawala Defence University, Werahera, Sri Lanka

<sup>3</sup>Department of Radiology, Juntendo University Shizuoka Hospital, Japan

### Corresponding author:

Sachila Niroshani, Department of Radiological Sciences, Graduate School of Human Health Sciences, Tokyo Metropolitan University, 7-2-10, Higashiogu, Arakawa-ku, Tokyo 116-8551, Japan.  
Email: [sachilahn@gmail.com](mailto:sachilahn@gmail.com)



Creative Commons Non Commercial CC BY-NC: This article is distributed under the terms of the Creative Commons Attribution-NonCommercial 4.0 License (<https://creativecommons.org/licenses/by-nc/4.0/>) which permits non-commercial use, reproduction and distribution of the work without further permission provided the original work is attributed as specified on the SAGE and Open Access pages (<https://us.sagepub.com/en-us/nam/open-access-at-sage>).

low-energy and high-energy levels by using different target filter combinations.<sup>6,7</sup> Low-energy (LE) and high-energy (HE) images are obtained after the administration of iodine-based contrast media intravenously.<sup>8</sup> These two images are recombined to create a final image, known as recombined image which clearly demonstrates contrast-enhanced mass within the breast due to different contrast enhancement within the normal breast tissues and the tumor areas.<sup>6,8</sup>

Low-energy images are acquired as standard mammograms with low energies which are below the k-edge of iodine (x-ray energy range from 26 kVp to 31 kVp).<sup>7,9</sup> LE images are similar to the 2-dimensional full-field digital mammography (2D-FFDM) and are used to interpret the structural changes of the breast.<sup>10</sup> HE images are acquired in the energy range 45–49 kVp to ensure that the x-ray beam energy is above the k-edge of iodine and demonstrate only contrast media uptake.<sup>11</sup> According to the previously published research, radiation dose to the breast is higher in complete DECEM due to the use of two exposures per view.<sup>12–15</sup> Yakoumakis et al. confirmed that the low-energy imaging mainly contributes to the total radiation dose received from the complete DECEM procedure.<sup>16</sup>

Only few studies are available regarding the optimization of radiation dose in CESM. A study conducted by Nishikawa et al. focused on the possibility of exposure dose reduction in CESM using dual-energy subtraction technique.<sup>17</sup> Phantom was used to optimize the scan protocol and parameter setting for reducing radiation dose without image degradation. They acquired the images using fully automated mode and manual mode and evaluated the image quality by image noise, contrast, and exposure dose. This study result reported that the average glandular dose (AGD) was able to reduce to 1.41 mGy from 1.96 mGy by setting manual mode. This study results suggested that it is possible to reduce the exposure dose by using manual mode instead of fully automated mode when performed CESM in clinical practice.

The aim of this research study is to use different combinations of energy levels for LE and HE images to make a recombined image and then assess the radiation dose received from the complete DECEM procedure without degrading the image quality of LE image and the final recombined image.

## Materials and Methods

The experiment was performed by using AMULET Innovality Fujifilm digital mammography machine with tungsten/rhodium (W/Rh) anode filter combination. A dedicated phantom, which is manufactured in Japan, was used for the experiment. As the first step, a 50% glandular–50% adipose, 50 mm thick phantom was used for exposures. The phantom consists of three slabs, and the middle main slab contains three different concentrations of iodine inserts.

Each iodine insert was 10 mm in diameter and concentration of 1.0 mgI/cm<sup>3</sup>, 2.0 mgI/cm<sup>3</sup>, and 4.0 mgI/cm<sup>3</sup>. LE images were obtained at 28 kVp, 30 kVp, and 32 kVp. HE images were acquired at 45 kVp, 47 kVp, and 49 kVp (Table 1). All exposures were made in manual mode. Different combinations of LE and HE images were used to create recombined images. LE image was subtracted from the HE image to create recombined images. Exposure was repeated for the 50 mm thickness 100% adipose and 50 mm thickness 100% glandular phantom to assess the dose reduction variations according to different breast equivalent compositions.

Mean glandular dose was calculated by using a method published by Dance et al.<sup>18</sup> Respective conversion coefficients were obtained by interpolating and extrapolating from the coefficients developed by Dance

$$\text{MGD} = k.g.c.s \quad (1)$$

where  $k$  is the incident air kerma at the upper surface of the breast without backscatter (IAK). IAK was measured by using semiconductor detector.  $g$  is the IAK to MGD conversion factor, and it corresponds to the glandularity of 50%.  $c$  factor corrects the differences from 50% glandularity, and  $s$ -factor corrects the differences from different target/filter combinations.

Image quality of LE and recombined images was calculated using the Fiji Image J software platform. The area of iodine inserts was selected as the region of interest (ROI) to calculate the mean pixel value of the iodine inserts (SI). The same ROI was used to measure the mean pixel value of the background (SB). Standard deviations (SD) for all ROI measurements of iodine inserts (I) and the background (B) were obtained. The CNR was calculated according to the equation given by the European mammography protocol.<sup>19</sup>

$$\text{CNR} = \frac{\text{mean pixel value}(SB) - \text{mean pixel value}(SI)}{\sqrt{\frac{SD(B)^2 + SD(I)^2}{2}}} \quad (2)$$

The FOM was calculated to evaluate the image quality with respect to the radiation dose delivered to the breast, and it is defined as follows

$$\text{FOM} = \frac{\text{CNR}^2}{\text{TMGD}} \quad (3)$$

where TMGD is the total mean glandular dose as the sum of individual doses from LE (MGD LE) and HE (MGD HE) images involved in the subtraction to make a recombined image

$$\text{TMGD} = \text{MGD}(LE) + \text{MGD}(HE) \quad (4)$$

total MGDs for three breast equivalent compositions were obtained by using 4<sup>th</sup> equation mentioned above.

## Results

The accurate *g* and *c* factors were calculated by interpolating and extrapolating of Dance’s coefficients.

*g*-factor calculation for LE exposure:

For 28 kV, 0.552 HVL, *g*-factor; 0.285,  
for 30 kV, 0.567 HVL, *g*-factor; 0.293, and  
for 32 kV, 0.584 HVL, *g*-factor; 0.302.

*g*-factor calculation for HE exposure:

For 45 kV, 0.699 HVL, *g*-factor; 0.367,  
for 47 kV, 0.709 HVL, *g*-factor; 0.373, and  
for 49 kV, 0.719 HVL, *g*-factor; 0.379.

*c*-factor of 50% fibroglandularity breast is 1.000 for any thickness of the breast while it varied for 100% adipose and 100% fibroglandular breasts.

*c*-factor for 50 mm, 100% adipose phantom LE exposure:

at 28 kV; 1.228,  
at 30 kV; 1.224, and  
at 32 kV; 1.220.

*c*-factor for 50 mm, 100% adipose phantom HE exposure:

at 45 kV; 1.182,  
at 47 kV; 1.178, and  
at 49 kV; 1.174.

**Table 1.** Exposure factors used for LE and HE imaging of 50 mm thickness 50% fibroglandular–50% adipose phantom.

LE		HE	
kVp	mAs	kVp	mAs
28	63	45	20
30	56	47	18
32	42	49	16

**Table 2.** MGD values of LE and HE images of 50 mm phantom with different compositions.

LE				HE			
kVp	MGD (mGy)			kVp	MGD (mGy)		
	50% glandular	100% adipose	100% glandular		50% glandular	100% adipose	100% glandular
28	0.91	0.77	1.29	45	0.88	0.68	1.27
30	0.88	0.56	1.22	47	0.86	0.54	1.22
32	0.86	0.54	1.19	49	0.84	0.52	1.17

Dance reported *s*-factor for W/Rh target/filter combination which was 1.042.

Calculated mean MGD values of LE, HE, and recombined images are summarized in Table 3 and Table 4

The CNR was assessed to determine the optimum tube voltage combination to make a recombined image (Table 5.) The CNR versus iodine concentration of iodine inserts on recombined images was plotted to estimate the accurate iodine concentration needed for required CNR value.

Measured CNR values of LE images are summarized in Table 6 according to different breast tissue equivalent compositions for the 50 mm thickness phantom. CNR values of recombined images were lower than that of the LE images. An increase in tube voltage leads to a decrease in CNR. Therefore, CNR values obtained in LE images were high compared to recombined images. CNR values obtained for recombined images are not lowering the image quality when compared to Dromain et al., 2014.<sup>20</sup>

In the present study, FOM values were not given relevant to 0 mGy and reported values given for the estimated total MGD values. FOM of the recombined images was plotted as a function of tube voltage used for HE exposure. Graphs were plotted for three different breast equivalent compositions to demonstrate the variation of FOM values according to different breast equivalent compositions. Each line plotted on the graph corresponds to the tube voltages used for LE exposure

## Discussion

Dual-energy contrast-enhanced mammography is the most promising technique in contrast imaging of the breast since it is less sensitive to patient motion. DECEM takes the advantage of differential attenuation of x-rays between breast tissues and iodine according to their mass attenuation coefficient. Mass attenuation coefficient of soft tissue and iodine is significantly different for the LE and HE spectra. Therefore, dual-energy technique can clearly discriminate the normal breast tissue and the tumor. According to Daniaux et al.,<sup>21</sup> the tube voltage used for LE imaging

**Table 3.** Total MGD values of recombined images according to different phantom compositions.

Recombined image LE + HE (kVp)	MGD (mGy)		
	50% glandular	100% adipose	100% glandular
28 + 45	1.79	1.45	2.56
28 + 47	1.77	1.31	2.51
28 + 49	1.75	1.29	2.46
30 + 45	1.76	1.24	2.49
30 + 47	1.74	1.10	2.44
30 + 49	1.72	1.08	2.39
32 + 45	1.74	1.22	2.46
32 + 47	1.72	1.08	2.41
32 + 49	1.70	1.06	2.36

**Table 4.** Calculated CNR values of three iodine inserts with different concentrations of recombined images.

Tube voltage combination for recombined image (LE image + HE image) kVp	CNR								
	100% adipose			50% adipose–50% fibroglandular			100% fibroglandular		
	Iodine concentration (mg/cm <sup>3</sup> )								
	1.0	2.0	4.0	1.0	2.0	4.0	1.0	2.0	4.0
28 + 45	0.45	0.88	1.63	1.06	1.42	2.40	0.84	1.45	2.59
28 + 47	–0.04	0.60	1.14	0.74	1.25	2.23	0.74	1.43	2.61
28 + 49	0.08	0.66	1.36	0.54	1.07	2.10	0.53	1.28	2.42
30 + 45	1.36	1.68	2.59	0.63	0.96	1.91	0.62	1.20	2.34
30 + 47	0.78	1.33	1.97	0.31	0.81	1.70	0.42	1.09	2.26
30 + 49	0.86	1.35	2.17	0.17	0.68	1.65	0.34	1.04	2.22
32 + 45	1.10	1.40	2.30	0.79	1.10	2.05	0.52	1.07	2.16
32 + 47	0.56	1.10	1.75	0.50	0.98	1.89	0.43	1.04	2.15
32 + 49	0.63	1.11	1.92	0.30	0.80	1.77	0.30	0.98	2.08

**Table 5.** CNR of iodine inserts of a 50% fibroglandular–50% adipose 50 mm thickness phantom-LE images.

kVp (LE image)	CNR								
	100% adipose			50% adipose–50% fibroglandular			100% fibroglandular		
	Iodine concentration (mg/cm <sup>3</sup> )								
	1.0	2.0	4.0	1.0	2.0	4.0	1.0	2.0	4.0
28	5.69	6.29	6.81	5.36	5.95	6.42	5.35	5.68	6.34
30	4.82	5.13	5.65	5.66	6.07	6.56	5.26	5.55	6.07
32	4.74	5.09	5.59	5.22	5.61	6.18	4.97	5.16	5.87

should be below the k-edge of iodine. Since the radiation dose from this dual-energy technique is higher than the FFDM, LE imaging is mainly contributing to the total radiation dose. Present study used different tube voltage values for LE and HE imaging and then reconstructed the

final image by using different combinations of kVp to assess the MGD and image quality quantitatively (Table 1 and Table 2).

The minimum MGD was observed with 32 kVp LE + 49 kVp HE (1.70 mGy) while the maximum was observed

**Table 6.** Different combinations of kVp used to create recombined images in the study.

Recombined image
LE + HE (kVp)
28 + 45
28 + 47
28 + 49
30 + 45
30 + 47
30 + 49
32 + 45
32 + 47
32 + 49

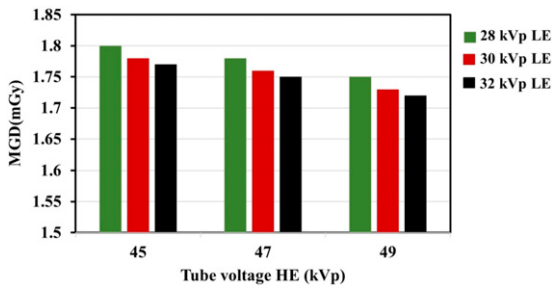


**Figure 1.** Total MGD of complete dual-energy contrast-enhanced mammography for 50 mm thickness, 50% fibroglandular–50% adipose phantom at different kVp combinations.

with 28 kVp + 45 kVp HE (1.79 mGy) for 50 mm thickness 50% fibroglandular phantom. The tube voltage combinations which gave minimum and maximum mean MGD for 100% adipose and 100% glandular phantom were the same as for 50% fibroglandular phantom (Table 3 and Table 4 and Figure 1). The maximum CNR value (2.40) was observed with 4.0 mgI/cm<sup>3</sup> iodine insert of 50% fibroglandular phantom for 28 kVp LE + 45 kVp HE voltage combination. But, CNR was highest (2.59) with 4.0 mgI/cm<sup>3</sup> iodine insert of the 100% adipose phantom for 30 kVp LE + 45 kVp HE while CNR was highest (2.61) with 4.0 mgI/cm<sup>3</sup> iodine insert of the 100% fibroglandular phantom for 30 kVp LE + 45 kVp HE (Table 5).

The CNR values of the iodine inserts in recombined images were decreased with increasing the selected tube voltage for LE and HE imaging. Hence, the total MGD increased 53% and 29% when using 28 kVp LE + 45 kVp HE and 28 kVp LE + 49 kVp HE compared to the highest kVp combination (32 kVp LE + 49 kVp HE) for 50% fibroglandular phantom, respectively (Table 3 and Table 4). Although LE images consist of iodine, they are similar to the 2D-FFDM images. Therefore, LE images should meet the optimum image quality standards. According to the

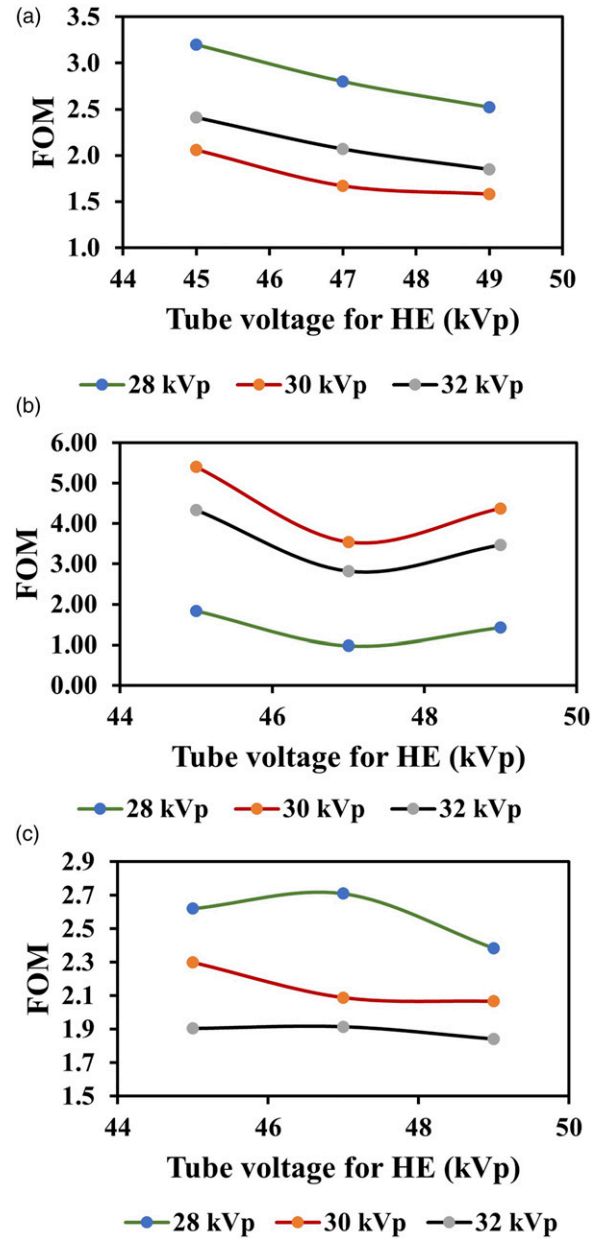


**Figure 2.** Figure of merit (FOM) values of 4.0 mgI/cm<sup>3</sup> iodine inserts of a 50 mm thickness (a) 50% fibroglandular–50% adipose, (b) 100% adipose, and (c) 100% glandular phantom recombined images.

results of Table 6, maximum CNR values were observed at 30 kVp for 50% fibroglandular phantom. The CNR values between 28 kVp and 30 kVp were not significantly different, and all those values are within the standard range as mentioned in Toroi et al.<sup>22</sup>. Therefore, it is possible to use 28 kVp or 30 kVp to obtain LE images of 50% fibroglandular standard breast. However, to increase the sensitivity of the recombined image, the optimum kVp for the LE image of 50% fibroglandular phantom is 28 kVp. However, to keep the radiation dose to the breast as

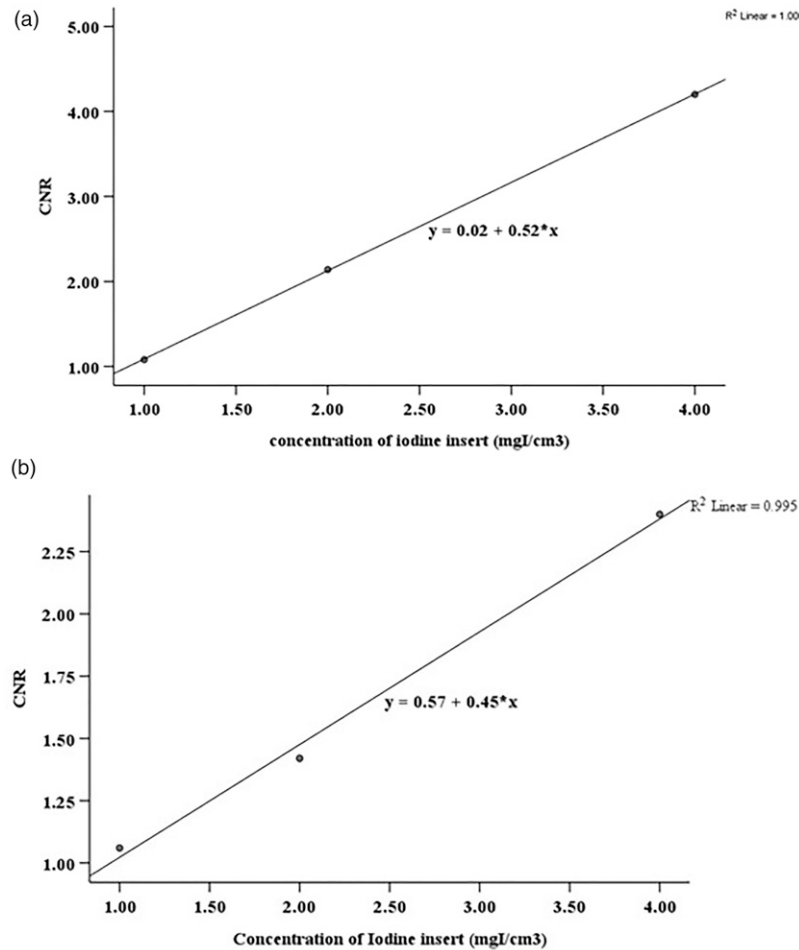


**Figure 3.** Contrast to noise ratio (CNR) as a function of the concentration of iodine inserts of the recombined image (a) 28 kVp LE + 49 kVp HE optimized voltage combination and (b) 28 kVp LE + 45 kVp HE voltage combination which gives the highest CNR.

low as possible, it is better to use the highest kVp to obtain HE images (49 kVp). Hence, 28 kVp + 49 kVp tube voltage combination produced recombined images without the loss of CNR with less dose increasing (29%) compared to the radiation dose received from 32 kVp LE + 49 kVp HE.

The study results for the 50% fibroglandular phantom confirmed that the FOM value reduced gradually with increasing HE tube voltage for each LE tube voltage and maximum values reported with 28 kVp LE tube voltage (Figure 2(a)–(c)). According to the t-test results ( $p > .05$ ), FOM values at 45 kVp and 49 kVp HE were not significantly different for any of the LE tube voltages. Therefore, FOM results of recombined images confirmed to use the 28 kVp LE + 49 kVp HE for the standard 50% fibroglandular phantom to reduce the radiation dose without degrading the image quality.

Although maximum CNR was observed with 30 kVp LE + 45 kVp HE for 100% adipose phantom, the radiation dose can be reduced by 11% and 13% when using 30 kVp LE + 47 kVp

HE and 30 kVp LE + 49 kVp HE, respectively, without the loss of image quality. FOM values for 100% adipose phantom were high at 30 kVp LE imaging. Radiation dose for 100% glandular phantom at 28 kVp LE + 45 kVp HE and 28 kVp LE + 47 kVp HE exceeded the dose limit reported in European reference frame (EUREF) guidelines (Table 3). Although both CNR and the FOM values were high for the 28 kVp LE + 47 kVp HE combination, it is not possible to use for the 100% glandular phantom. Therefore, 32 kVp LE + 49 kVp HE with  $\geq 2.0$  mgI/cm<sup>3</sup> iodine concentration is the optimum combination for 100% glandular phantom (Table 4 and Figure 2c).

Pearson correlation test found that the CNR value of the iodine inserts in recombined images had a strong positive relationship with the concentration of iodine ( $r = 0.925$ ). It was found that a linear fit to the calculated CNR value of the iodine inserts of recombined images resulted in  $R^2$  values superior to the 0.99 (Figure 3) and it was comparable to the Dromain et al. According to Dromain et al., this linear fit can be used to detect minimal iodine concentration of a lesion by using Rose criteria<sup>20</sup>.



Our study has several limitations. The tube voltage optimization was done only for 50 mm thickness and three different breast equivalent phantoms. This evaluation should be extended to the clinically available range of breast thicknesses and breast glandularities before these tube voltages set it for clinical use. In addition, the study recommended to evaluate the LE image quality visually according to EUREF criteria for implication of practice.

In conclusion, the use of as low as possible tube voltage for the LE imaging of standard 50% fibroglandular breast while using the highest tube voltage for HE imaging has reduced the MGD while keeping optimum image quality. The best match between the radiation dose and image quality was found in the recombined images. Moreover, CESM procedure can be performed with  $\geq 2.0$  mgI/cm<sup>3</sup> iodine concentration to obtain a better CNR value in the recombined images of three breast compositions even at high voltages when radiation dose needs to be the main consideration.

### Acknowledgments

We gratefully acknowledge the staff of the mammography unit at the Juntendo University Shizuoka Hospital, Japan for their immense support.

### Declaration of Conflicting Interests

The author(s) declared no potential conflicts of interest with respect to the research, authorship, and/or publication of this article.

### Funding

The author(s) disclosed receipt of the following financial support for the research, authorship, and/or publication of this article: The first author was supported by Tokyo Human Resources Fund for City Diplomacy Scholarship. But no specific grants from funding agencies outside the University.

### Ethics Approval

Ethical committee approval is not required since this article does not contain any procedures involving human participants.

### ORCID iDs

Sachila Niroshani  <https://orcid.org/0000-0002-9705-9759>

Tokiko Nakamura  <https://orcid.org/0000-0003-2124-3186>

### References

- Kolb TM, Lichy J, Newhouse JH, et al. Comparison of the performance of screening mammography, physical examination, and breast US and evaluation of factors that influence them: an analysis of 27, 825 patient evaluations. *Radiology* 2002; 225: 165–175.
- Jong RA, Yaffe MJ, Skarpathiotakis M, et al. Contrast enhanced digital mammography: initial clinical experience. *Radiology* 2003; 228: 842–850.
- Diekmann F, Diekmann S, Jeunehomme F, et al. Digital mammography using iodine-based contrast media: initial clinical experience with dynamic contrast medium enhancement. *Invest Radiol* 2005; 40: 397–404.
- Diekmann F, Freyer M, Diekmann S, et al. Evaluation of contrast-enhanced digital mammography. *Eur J Radiol* 2011; 78: 112–121.
- Dromain C, Thibault F, Diekmann F, et al. Dual-energy contrast enhanced digital mammography: initial clinical results of a multireader, multicase study. *Breast Cancer Res* 2012; 14: 1–17.
- Dromain C, Balleyguier C, Adler G, et al. Contrast-enhanced digital mammography. *Eur J Radiol* 2009; 69: 34–42.
- Jochelson MS, Dershaw DD, Sung JS, et al. Bilateral contrast-enhanced dual-energy digital mammography: feasibility and comparison with conventional digital mammography and MR imaging in women with known breast carcinoma. *Radiology* 2013; 266: 743–751.
- Sorin V and Sklair-Levy M. Dual-energy contrast-enhanced spectral mammography (CESM) for breast cancer screening. *Quantitative Imaging Medicine Surgery* 2019; 9: 1914–1917.
- Skarpathiotakis M, Yaffe MJ, Bloomquist AK, et al. Development of contrast digital mammography. *Med Phys* 2002; 29: 2419–2426.
- Lalji UC, Jeukens CR, Houben I, et al. Evaluation of low-energy contrast-enhanced spectral mammography images by comparing them to full-field digital mammography using EUREF image quality criteria. *Eur Radiol* 2015; 25: 2813–2820.
- Lalji U and Lobbes M. Contrast-enhanced dual-energy mammography: a promising new imaging tool in breast cancer detection. *Wom Health* 2014; 10: 289–298.
- Dromain C, Thibault F, Muller S, et al. Dual-energy contrast-enhanced digital mammography: initial clinical results. *Eur Radiology* 2011; 21: 565–574.
- James JR, Pavlicek W, Hanson JA, et al. Breast radiation dose with CESM compared with 2D FFDM and 3D tomosynthesis mammography. *AJR Am J Roentgenol* 2017; 208: 362–372.
- Jeukens CR, Lalji UC, Meijer E, et al. Radiation exposure of contrast-enhanced spectral mammography compared with full-field digital mammography. *Invest Radiol* 2014; 49: 659–665.
- Badr S, Laurent N, Regis C, et al. Regis C, et al. Dual-energy contrast enhanced digital mammography in routine clinical practice in 2013. *Diagn Interv Imaging* 2014; 95: 245–258.
- Yakoumakis E, Tzamicha E, Dimitriadis A, et al. Dual-energy contrast-enhanced digital mammography: patient radiation dose estimation using a Monte Carlo code. *Radiat Protect Dosim* 2015; 165(1–4): 369–372.
- Nishikawa N, Yanagisawa K, Naoi K, et al. Possibility of exposure dose reduction in contrast enhanced spectral mammography using dual energy subtraction technique: a phantom study. In: Fujita H, Hara T, Muramatsu C (eds)

- Breast Imaging. IWDM 2014. Lecture Notes in Computer Science 2014. 2014. Cham: Springer, 8539.
18. Dance D, Skinner C, Young K, et al. Additional factors for estimation of mean glandular breast dose using the UK mammography dosimetry protocol. *Phys Med Biol* 2000; 45: 3225–3240.
  19. Amendoeira I, Perry N, Broeders M, et al. European Commission. S1 digital mammography update European guidelines for quality assurance in breast cancer screening and diagnosis. 4th ed. Luxembourg: EU publications, 2013.
  20. Dromain C, Canale S, Saab-Puong S, et al. Optimization of contrast-enhanced spectral mammography depending on clinical indication. *J Med Imag* 2014; 1: 033506.
  21. Daniaux M, De Zordo T, Santner W, et al. Dual-energy contrast-enhanced spectral mammography (CESM). *Arch Gynecol Obstet* 2015; 292: 739–747.
  22. Toroi P, Zanca F, Young KC, et al. Experimental investigation on the choice of the tungsten/rhodium anode/filter combination for an amorphous selenium-based digital mammography system. *Eur Radiol* 2007; 17: 2368–2375.